



## Assessment of the Approximate Non-linear Seismic Analysis Methods

El-Masry\*, S. S., Aboul Nour\*\*, L. A. and Fayed\*\*\*, M. N.

\*Ph.D., Structural Engineering Department, Faculty of Engineering, Zagazig University, Egypt

\*\*Associate prof., Structural Engineering Department, Faculty of Engineering, Zagazig University, Egypt

\*\*\* Prof., Structural Engineering Department, Faculty of Engineering, Ain Shams University, Egypt

### الملخص العربي

يهدف هذا البحث إلى تقييم طريقتين مستحدثتين من طرق التحليل بالدفع الجانبي الإستاتيكية للاخطية، و هي طريقة التحليل بالدفع الجانبي متعدد الأنماط (MPA) و طريقة (N2) و ذلك من خلال تطبيق هذا التحليل على اثنين من المباني الخرسانية المسلحة متعددة الطوابق و ذلك تحت تأثير أربعة من الزلازل و دراسة الاستجابات الزلزالية غير المرنة لكل مبنى، و التي تتضمن كلا من: الازاحة الجانبية لسطح المبنى، قوى القص عند القاعدة، الازاحة الكلية الجانبية للطوابق، و الازاحة الجانبية بين الطوابق، و التوزيعات المفصلية للدنة (الغير مرنة). و من ثم مقارنة جميع القيم المستنتجة مع ما يقابلها من قيم ناتجة عن تطبيق طريقة التحليل بالسجل الزمني للاخطية (NLTH) و التي تمثل أفضل و أصح طريقة للحصول على التنبؤات الأدق و الأكثر قربا للسلوك الفعلي الحقيقي للمنشأ. و قد تم تطبيقها على كل حالة من الحالات التي تم دراستها مرتين إحداهما باستخدام برنامج التحليل الإنشائي المعروف SAP2000 و الأخرى عن طريق عمل برمجة لخطواتها على برنامج MATLAB. من خلال هذا البحث، تم إثبات أن طرق التحليل بالدفع الجانبي الإستاتيكية للاخطية (MPA) و (N2) كلاهما طرق عالية الكفاءة كطرق تحليل عملية بديلة لطريقة ال (NLTH). كما تم دراسة تأثير تغيير أنماط الحمل الجانبي (Lateral Load Patterns) على نتائج طريقة (N2 method) من خلال استخدام خمس أنماط مختلفة و تطبيقها على المنشآت محل الدراسة.

### ABSTRACT

This paper presents comparison among different nonlinear seismic analysis methods, i.e. pushover analyses include: Modal pushover analysis (MPA) and N2 method, in addition to nonlinear dynamic analyses include: nonlinear time history (NLTH) methods by using both of Matlab and Sap2000 computer programs. The NLTH-sap2000 is considered the major method, while the rest methods are compared to it. The underlying concept of each studied nonlinear analysis method is outlined and step-by-step procedure is summarized. Applications have performed for two RC building frames. The accuracy and reliability of MPA and N2 in estimating the peak responses of the global and the local seismic demands is evaluated and compared with the same values resulted in the (NLTH) analyses methods. Based on that N2 method is considered a practical alternative method for the nonlinear time-history analysis, the effect of the applied lateral load pattern type by the N2 method is studied by exploring five different types. NLTH programming in MATLAB is introduced for tending to future studies with acceptable accuracy in the use of diverse parameters. The results are presented and discussed.

**Keywords:** Modal Pushover Analysis; Nonlinear Time History; Seismic demands; Roof drift; Base shear ratio; Inter-story drift ratio and plastic hinges.

### 1. INTRODUCTION

By the last decade, it is increased the need to the determination and evaluation of the damages in the building type of structures due to the frequent earthquakes. The most destructive and unfortunately the most general irregularity in Egyptian stock of building structures that lead to collapse is certainly the reinforced concrete (RC) frames. In order

to prevent such collapse mechanisms in the building structures, seismic demands must be determined accurately. For this reason, many evaluation and retrofiting methods are proposed for the accurate determination of the inelastic behaviors and seismic demands of the building structures. Furthermore, the earthquake codes of many countries such as the recent world Earthquake Codes recommend these methods in the analysis of the buildings. There are two common methods, which are based on the nonlinear static pushover analysis. Capacity Spectrum Method, which is also referred in ATC-40 (1996). It was developed by Freeman et.al. (1993). In the method, the structural capacity curve is calculated and compared with the demand spectrum to get on a performance point for performance evaluation of the structure. The second method, Displacement Coefficient Method that is described in FEMA-356 (2000), is based on the displacement modification factors used for modifying the elastic spectral displacement of an equivalent SDOF system. The approximations made for these methods bring some weaknesses such as not considering the higher mode effects and invariant lateral load patterns. In the literature, many researchers investigated and tried to improve these weaknesses. For example, (Fajfar and Fischinger 1987) offered using invariant story forces proportional to the deflected shape of the structure. (Eberhard and Sözen 1993) offered load patterns based on mode shapes derived from secant stiffness at each load step.

Pushover analysis is a static technique that directly involves the nonlinear properties of materials (Mazza, 2014; Poursha et al. 2014) investigated by many researchers for various structures (e.g. Nguyen et al., 2010; Khoshnoudian and Kashani, 2012; Malekzadeh, 2013; Panyakapo, 2014). Conventional pushover methods apply an increasingly single direction predetermined load pattern which is kept constant throughout the analysis (EN, 2004; FEMA, 2005; Camara and Astiz, 2012; Manoukas et al., 2012; Giorgi and Scotta, 2013; Beheshti-Aval and Keshani, 2014). Several studies confirmed by the fact that the simplified procedures based on invariant load patterns are partially inadequate to predict inelastic seismic demands in buildings when the issues such as effects of higher modes, inelastic effects, and cumulative damages are significant (Shakeri et al., 2012; Abbasnia et al., 2013; Kunnath and Kalkan, 2004). Nonlinear time history analysis (NTHA) is known as the most accurate method to evaluate the response of the structures subjected to earthquake excitations. Nevertheless, some of the nonlinear static procedures (NSPs) are still popular for assessing the seismic capacity of structures due to their simplicity and application (Jiang et al. 2010; Amini and Poursha, 2016; Izadinia et al., 2012).

The main objectives of this study is the evaluation of the accuracy and efficiency of the nonlinear static pushover analyses include: MPA which considers various calculated lateral load patterns based on the first three “modes” of every studied frame and N2 which calculates one lateral load pattern based on only the first “mode” of every studied frame, In addition to support this evaluation by the nonlinear time history analyses. Two-dimensional reinforced concrete analytical models are formed and designed according to the current Egyptian codes (ECP-203 and ECP-201), and then evaluated by utilizing the studied nonlinear analyses. The results include estimating the peak responses of the global seismic demands; roof drift ratio ( $\Delta_{\max}/H$ ) & base shear ( $V_{b\max}$ ) and the local seismic demands; the inter-story drift ratio (IDR) & floor displacement profiles (FDP). In addition to evaluate and compare the general shape of the deformed plastic hinges of the studied building structures.

## 2. NONLINEAR ANALYSIS METHODS

### 2.1 Nonlinear Time History Analysis (NLTH) Using Matlab Program

The analysis here is carried out by a step-by-step numerical integration of the differential equations of motion (Mario and William 2003). The proposed method of analysis is based on the stiffness method as explained in the following flow chart, (Fig 1), using both of the elastic plastic model and the hardening plastic hinge model. The Matlab computer program is used to determine the response of the framed structures in the elastic and plastic ranges under the earthquake excitation.

At the end of each step interval it is necessary to calculate the end moments of every beam segment to check whether or not a plastic hinge has been formed. The calculation is done using the element incremental moment - displacement relationship. It is also necessary to check if the plastic deformation associated with a hinge is compatible with the sign of the moment.

The assumed moment rotation characteristics of the member are of the type illustrated in fig. 2. The conditions implied by this model are: (1) the moment cannot exceed the plastic moment; (2) if the moment is less than the plastic moment, the hinge cannot rotate; (3) if the moment is equal to the plastic moment, then the hinge may rotate in the direction consistent with the sign of the moment; (4) if the hinge starts to rotate in a direction inconsistent With the sign of the moment, the hinge is removed.

The incremental rotation of a plastic hinge is given by the difference between the incremental joint rotation of the frame and the increase in rotation of the end of the member at that joint. For example, with a hinge at end I only, fig 3, the incremental joint rotation is  $\Delta\delta_2$  and the increase in rotation of this end due to rotation  $\Delta\delta_4$  is  $-\Delta\delta_4/2$  and that due to the displacements  $\Delta\delta_1$  and  $\Delta\delta_3$  is  $1.5(\Delta\delta_3 - \Delta\delta_2)/L$ . Hence the increment in rotation  $\Delta\rho_i$  of a hinge formed at end I is given by equation (1). Similarly, with a hinge formed at end J only, the increment in rotation of this hinge is given by equation (2). Finally, with hinges formed at both ends of a beam segment, the rotations of the hinges are given by equations (3) and (4).

$$\Delta\rho_i = \Delta\delta_2 + \frac{1}{2} \Delta\delta_4 - 1.5 \frac{\Delta\delta_3 - \Delta\delta_1}{L} \quad \Delta\rho_j = \Delta\delta_4 + \frac{1}{2} \Delta\delta_2 - 1.5 \frac{\Delta\delta_3 - \Delta\delta_1}{L} \quad (1, 2)$$

$$\Delta\rho_i = \Delta\delta_1 - \frac{\Delta\delta_3 - \Delta\delta_1}{L} \quad \Delta\rho_j = \Delta\delta_3 - \frac{\Delta\delta_3 - \Delta\delta_1}{L} \quad (3, 4)$$

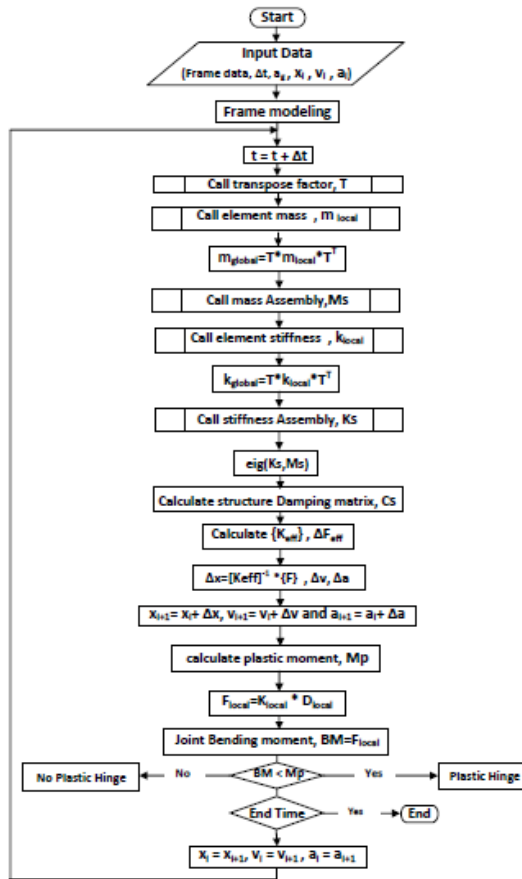


Fig.1 flow Chart

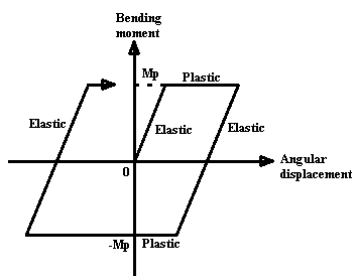


Fig.2 Elastoplastic relationship between bending moment and angular displacement at a section of a beam.

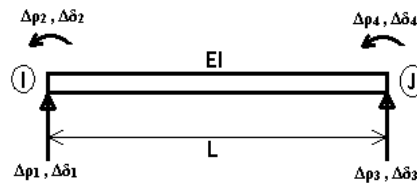
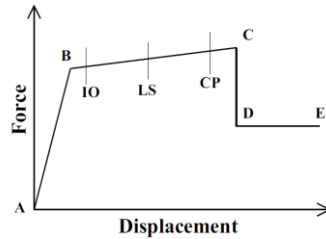


Fig.3 Beam segment indicating incremental end forces and corresponding incremental displacements.

## 2.2 NLTHA and P.O.A Concepts in Sap2000 Program

### (a) Nonlinear Properties

It is might insert plastic hinges at any number of locations along the clear length of the element. Detailed description of the behavior and use of plastic hinges is presented in the following paragraphs.



**Fig. 4:** The A-B-C-D-E curve for Force vs. Displacement or Moment vs. Rotation.

### (b) Plastic Deformation Curve

For each degree of freedom, it is defined a force-displacement (moment-rotation) curve that gives the yield value and the plastic deformation following yield. This is done in terms of a curve with values at five points, A-B-C-D-E, as shown in fig. 4.

- Point A is always the origin.
- Point B represents yielding. Only the plastic deformation beyond point B will be exhibited by the hinge.
- Point C represents the ultimate capacity for pushover analysis.
- Point D represents a residual strength for pushover analysis.
- Point E represents total failure.

Additional deformation are measured at points IO (immediate occupancy), LS (life safety), and CP (collapse prevention). These are informational measured that are reported in the analysis results and used for performance-based design. Prior to reaching point B, all deformation is linear and occurs in the Frame element itself, not the hinge. Plastic deformation beyond point B occurs in the hinge in addition to any elastic deformation that may occur in the element. When the hinge unloads elastically, it does so without any plastic deformation, i.e., parallel to slope A-B. The built-in automatic hinge properties for concrete members are based on Tables 6-7 and 6-8 in FEMA-356 (2000).

### 2.3 Nonlinear Time History Analysis (NLTHA) Using SAP2000 Program

In SAP2000, the nonlinear time-history analysis can be carried out as follows (Altuntop, 2007):

- The model representing the building structure is created and vertical loads (dead load and live load), member properties and member nonlinear behaviors are defined and assigned to the model.
- Floor masses are assigned to the model.
- Hinge properties are defined and these properties are assigned to the member ends considering end-offsets.
- The ground motion record is defined as a function of acceleration versus time.
- An initial loading is applied to the model to represent the initial case. This case must be composed of the dead loads and reduced live loads.

In this study, direct integration method is used for the analyses ('Hilbert-Hughes-Taylor alpha' method considering the variant alpha values between 0 and -1/3)

### 2.4 Modal Pushover Analysis (MPA)

#### (a) Basic Concept

The equations of motion for a symmetric-plan multistory building subjected to earthquake ground acceleration  $\ddot{u}_g(t)$  are the same as those for external forces, known as the effective earthquake forces (Chopra, 2003):

$$\mathbf{p}_{\text{eff}}(t) = -\mathbf{m}\mathbf{1}\ddot{u}_g(t) \quad (5)$$

where  $\mathbf{m}$  is the mass matrix and  $\mathbf{1}$  is a vector with all elements equal to unity. Defined by  $\mathbf{s} \equiv \mathbf{m}\mathbf{1}$ , the spatial (height wise) distribution of forces can be expanded into its modal components  $\mathbf{s}_n$  :

$$\mathbf{s} = \sum_{n=1}^N \mathbf{s}_n \quad \mathbf{s}_n \equiv \Gamma_n \mathbf{m} \boldsymbol{\phi}_n \quad (6)$$

$$\Gamma_n = \boldsymbol{\phi}_n^T \mathbf{m} \mathbf{1} / \boldsymbol{\phi}_n^T \mathbf{m} \boldsymbol{\phi}_n \quad (7)$$

where  $\boldsymbol{\phi}_n$  is the nth-mode.

In the MPA procedure, the peak response of the building to  $\mathbf{p}_{\text{eff},n}(t) = -\mathbf{s}_n \ddot{u}_g(t)$ , the nth-mode component of effective forces, is determined by a nonlinear static or pushover analysis. The peak demands due to these modal components of forces are then combined by an appropriate modal combination rule.

#### (b) Summary of Procedure

The MPA procedure, which has been developed by Chopra and Goel (2003) to consider the contributions of higher modes of vibration, is summarized below in a sequence of steps:

1. Compute the natural periods,  $T_n$ , and modes,  $\boldsymbol{\phi}_n$ , for linearly-elastic vibration of the building.
2. Develop the base-shear–roof-displacement ( $V_{bn} - u_{rn}$ ) pushover curve for the nth-mode force distribution  $\mathbf{s}_n^* = \mathbf{m} \boldsymbol{\phi}_n$ . Gravity loads, including those acting on the interior (gravity) frames, are applied before the first-“mode” pushover analysis. The resulting P- $\Delta$  effects generally lead to a pushover curve with negative post-yield stiffness. The gravity loads are not considered in developing the higher-mode pushover curves.
3. Idealize the pushover curve as a bilinear curve.
4. Convert the idealized pushover curve to the force-deformation ( $F_{sn}/L_n - D_n$ ) relation of the nth-“mode” inelastic SDF system by utilizing the relationships

$$\frac{F_{sny}}{L_n} = \frac{V_{bny}}{M_n^*} \quad D_{ny} = \frac{u_{rny}}{\Gamma_n \phi_{rn}} \quad (8, 9)$$

Where  $M_n^*$  is the effective modal mass, and  $\phi_{rn}$  is the nth-mode shape value at the roof.

5. Compute the peak deformation,  $D_n$  of the nth-“mode” inelastic SDF system with force-deformation relation and damping ratio  $\zeta_n$ . The initial vibration period of the system is  $T_n = (2\pi L_n D_{ny} / F_{ny})^{1/2}$ . For a SDF system with known  $T_n$ ,  $\zeta_n$ , and force-deformation relation,  $D_n$  for a given ground motion can be computed by nonlinear

RHA. In practical application,  $D_n$  would be estimated from a design spectrum using empirical equations for inelastic deformation ratios.

6. Calculate the peak roof displacement  $u_{rn}$  associated with the  $n$ th-“mode” inelastic SDF system from

$$u_{rn} = \Gamma_n \phi_{rn} D_n \quad (10)$$

7. From the pushover database values at roof displacement  $u_{rn}$ , extract values of desired response  $r_n$ : floor displacements, story drifts, plastic hinge rotations, etc.

8. Repeat Steps 3 to 7 for as many “modes” as required for sufficient accuracy; usually the first two or three “modes” will suffice.

9. Determine the total response (demand)  $r_{MPA}$  by combining the peak “modal” responses using an appropriate modal combination rule, e.g., the SRSS combination rule:

$$r_{MPA} = \left( \sum_{n=1}^J r_n^2 \right)^{1/2} \quad (11)$$

where  $J$  is the number of “modes” included.

## 2.5 N2 method

N2 method is a nonlinear analysis method that introduces a combination of nonlinear static pushover analysis and the response spectrum approach for performance based seismic design. The N2 method steps are listed as follows:

### 2.5.1 Getting capacity curve for the nonlinear MDOF model

Pushover analysis is performed by subjecting the MDOF model to an increasing pattern of an assumed lateral load. Since, it is applied the following steps, Fajfar (2000):

(a) Assume displacement shape ( $\Phi$ ), (b) Determine vertical distribution of lateral forces.

$$\{P\} = [M] \{\Phi\}, \quad P_i = m_i \Phi_i \quad (12)$$

(c) Determine base shear ( $V$ )- top displacement ( $D_t$ ) relationship.

### 2.5.2 Getting equivalent SDOF model and its capacity curve

(1) getting the modal participation factor and (2) divide the MDOF quantities ( $V$ ,  $D_t$ ) by the modal participation factor ( $\Gamma$ ). (3) Determine the capacity diagram in AD format. (4) Determine the elastic period of the idealized bilinear system  $T^*$ .

$$\Gamma = \frac{\sum m_i \Phi_i}{\sum m_i \Phi_i^2} = \frac{m^*}{\sum m_i \Phi_i^2} \quad D^* = \frac{D_t}{\Gamma} \quad F^* = \frac{V}{\Gamma} \quad (13, 14, 15)$$

$$S_a = \frac{F^*}{m^*} \quad T^* = 2\pi \sqrt{\frac{m^* D_y^*}{F_y^*}} \quad (16, 17)$$

Where:  $m_i$ : is the mass of the  $i$ th story,  $m^*$ : is the equivalent mass of the SDOF system.

$\Phi$ : is the assumed displacement shape.

$F_y$  and  $D_y^*$ : are the yield strength and displacement, respectively.

### 2.5.3 Specifying seismic elastic demand spectrum in A-D format

Determining the displacement for an elastic SDOF system by the following relation

$$S_{de} = \frac{T_f^2}{4\pi^2} S_{ae} \quad (18)$$

Where  $S_{de}$  and  $S_{ae}$ : are the displacement and acceleration of an elastic response spectrum corresponding to the fundamental period  $T_f$  and a viscous damping ratio, respectively.

### 2.5.4 Converting the elastic demand spectrum into inelastic damped demand spectrum.

(1) Determining the ductility reduction factor  $R_\mu$ , see (Fig.6):

$$R_\mu = \frac{S_{ae}(T_f)}{S_{ay}} \quad (19)$$

Where,  $S_{ay}$ : The acceleration of the inelastic system.

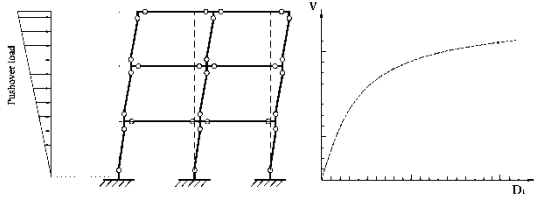


**Fig. 5:** Pushover analysis.

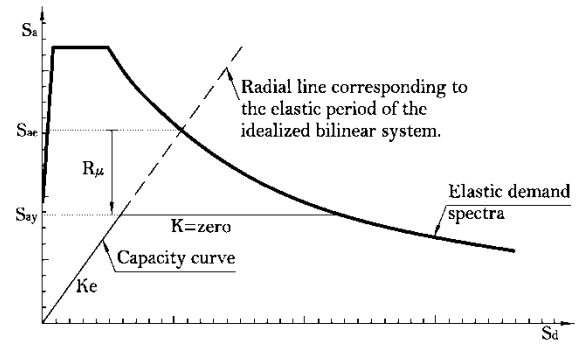


**Fig. 6:** Idealized capacity curve with elastic demand spectrum, showing how to obtain  $R_\mu$ .

(2) Determine the inelastic displacement demand for an inelastic SDOF system. Where,  $\mu$  is the ductility demand.

$$S_d = \mu S_{dy} \quad \text{or} \quad S_d = \frac{\mu}{R_\mu} S_{de} \quad (20, 21)$$

$$\mu = (R_\mu - 1) \frac{T_c}{T_f} + 1 \quad T_f < T_c \quad (22)$$

$$\mu = R_\mu \quad T_f \geq T_c \quad (23)$$

Where  $T_c$  is the characteristic period of the ground motion, consequently, (3) calculating the inelastic displacement demand.

$$S_d = \frac{S_{de}}{R_\mu} \left( 1 + (R_\mu - 1) \frac{T_c}{T^*} \right) \quad T^* < T_c \quad (24)$$

$$S_d = S_{de} \quad T^* \geq T_c \quad (25)$$

### 2.5.5 Getting global and local seismic demand for the MDOF model

Transform the SDOF inelastic displacement demand to the maximum top displacement  $D_t$  of the MDOF system (target displacement) by:

$$D_t = \Gamma S_d \quad (26)$$

The local seismic demand can be determined by a pushover analysis under increasing lateral loads to its target top displacement.

## 2.6 Study the Effect of the L.L.P Type

A parametric study is carried out to investigate the effect of the applied lateral load pattern type through the N2 method procedure, on the inelastic seismic responses of the studied RC building frames (6 and 12 stories).

### 2.6.1 The Studied Lateral Load Patterns Types

Five different load patterns are briefly explained in the following sections:

1. Code Lateral Load Pattern, Egyptian Code ECP-201 (2012).

$$F_i = \left[ \frac{z_i W_i}{\sum_{j=1,n} z_j W_j} \right] \cdot F_b \quad (27)$$

In the above equation,  $F_b$  is the total base shear;  $z_i$  is the height of  $i$ -th story above the base,  $n$  is the total number of stories and  $W_i$  is the weight of the  $i$ -th story.

2. Uniform Lateral Load Pattern

The lateral force at any story is calculated by the following formula:

$$F_i = \frac{w_i}{\sum_1^N w} * V_t \quad (28)$$

$V_t$  is the total base shear obtained by the effective first mode forces,  $w_i$  is the weight of the  $i$ -th story and  $N$  is the number of stories.

3. Elastic First Mode Lateral Load Pattern

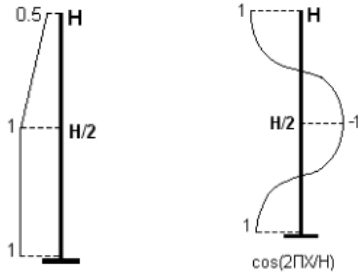
The lateral force at any story is formulated as follows:

$$F_i = m_i \Phi_i / \sum_1^N m_i \Phi_i \quad (29)$$

Where,  $\Phi_i$  is the amplitude of the elastic first mode at  $i$ -th story and  $m_i$  is the mass at  $i$ -th story.

4. Proposed Types of Lateral Load Patterns

It has been proposed two types of lateral load patterns to appear as these shown configurations



Where, both types' functions depend on the height (H) of the studied frame as shown.

### 3- THE BUILDINGS CHARACTERISTICS

Two residential buildings are symmetrical and square in plane as shown in Figs. 9 and 10, where the structural system is described by reinforced concrete (RC) moment-resisting frames. The selected numbers of stories are 6 and 12 stories, and the selected number of bays is 3 bays, Abd-El-Wahab (2008). These two RC buildings are designed in accordance with the Egyptian code for design and construction of RC structures, ECP-203 (2007), and the design loads are determined according to Egyptian code for calculating loads and forces in structural work and masonry, ECP-201 (2012). Tables 1 and 2 list the dimensions and reinforcement of the beams and columns for each of the two RC building frames.

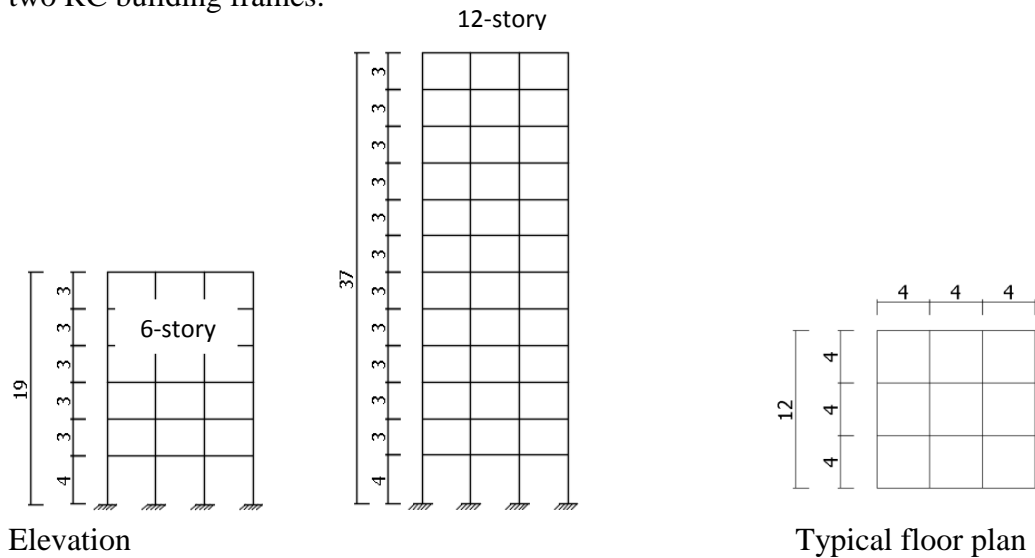


**Fig. 9:** Layout of studied buildings

**Table 1:** Dimensioning and reinforcement of 6-story, 3-bay RC frame

		Story Number	
		1, 2, 3	4, 5, 6
Beams	Cross Section (m <sup>2</sup> ) Reinforcement (Top & Bottom)	0.25 X 0.50 4 $\phi$ 16	0.25 X 0.50 4 $\phi$ 16
Edge Columns	Cross Section (m <sup>2</sup> ) Reinforcement Stirrups	0.25 X 0.80 10 $\phi$ 16 5 $\phi$ 10 /m	0.25 X 0.70 10 $\phi$ 16 5 $\phi$ 10 /m
Inner Columns	Cross Section (m <sup>2</sup> ) Reinforcement Stirrups	0.60 X 0.60 20 $\phi$ 16 5 $\phi$ 10 /m	0.50 X 0.50 16 $\phi$ 16 5 $\phi$ 10 /m

**Table 2:** Dimensioning and reinforcement of 12-story, 3-bay RC frame

		Story Number			
		1, 2, 3	4, 5, 6	7, 8, 9	10,11,12
Beams	Cross Section (m <sup>2</sup> ) Reinforcement (Top & Bottom)	0.25 X 0.70 4 $\phi$ 16	0.25 X 0.50 4 $\phi$ 16	0.25 X 0.50 4 $\phi$ 16	0.25 X 0.50 4 $\phi$ 16
Edge Columns	Cross Section (m <sup>2</sup> ) Reinforcement Stirrups	0.25 X 1.00 14 $\phi$ 16 5 $\phi$ 10 /m	0.25 X 0.90 12 $\phi$ 16 5 $\phi$ 10 /m	0.25 X 0.80 10 $\phi$ 16 5 $\phi$ 10 /m	0.25 X 0.70 10 $\phi$ 16 5 $\phi$ 10 /m
Inner Columns	Cross Section (m <sup>2</sup> ) Reinforcement Stirrups	0.80 X 0.80 28 $\phi$ 16 5 $\phi$ 10 /m	0.70 X 0.70 24 $\phi$ 16 5 $\phi$ 10 /m	0.60 X 0.60 20 $\phi$ 16 5 $\phi$ 10 /m	0.50 X 0.50 16 $\phi$ 16 5 $\phi$ 10 /m

#### 4. EARTHQUAKE RECORDS

The RC building frames, which are described in the past section, are analyzed under the seismic action of the earthquakes: Altadena, Corralit, Pomona and Lacc-Nor. The acceleration –time history of these earthquakes are shown in Fig. 11. The peak ground acceleration (PGA) is equal to 0.438g for Altadena, 0.617g for Corralit, 0.182g for Pomona, and 0.217g for Lacc-Nor, where g refers to the gravity acceleration (i.e.,  $g=9.81 \text{ m/s}^2$ ). These earthquake records have been scaled to be consistence with seismic zone intensity 0.15g.

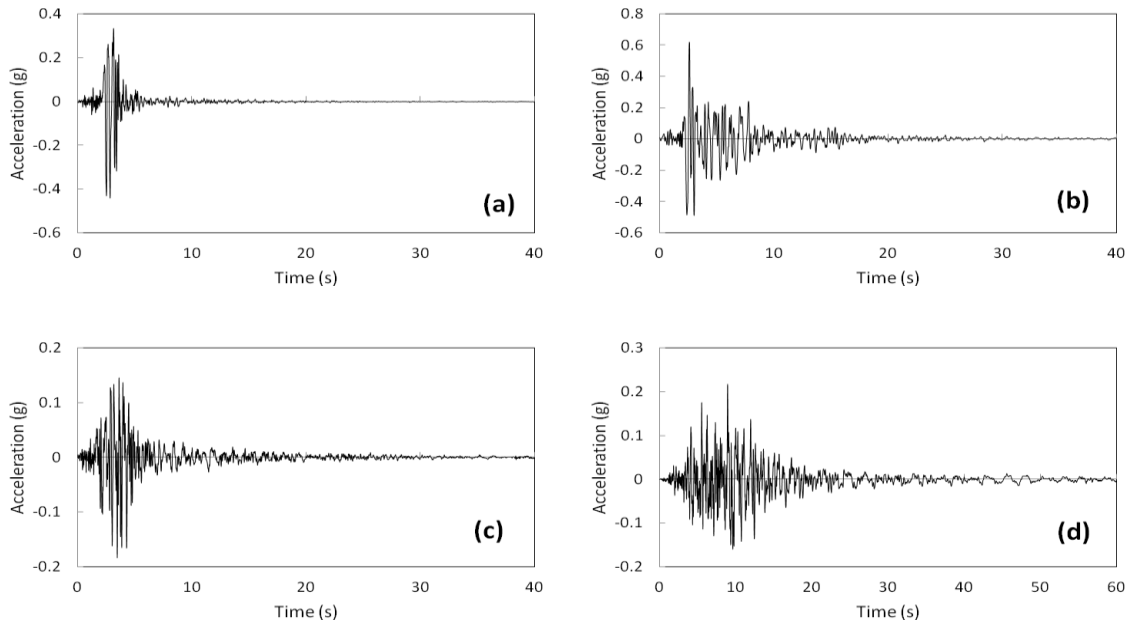


**Fig.11:** Acceleration – time history records of (a) ALTADENA, (b) CORRALIT, (c) PONOMA and (d) LACC-NOR earthquakes.

#### 5. EVALUATION AND COMPARISON

##### 5.1 Characteristics of Modal Pushover Analysis (MPA)

The following seismic demands are estimated by the MPA method of the 6-story and 12-story RC building frames under the seismic action of Altadena, Corralit, Pomona and Lacc-Nor earthquakes.

### 5.1.1 Target drift ratio and base shear

It is more convenient to use the target drift ratio ( $\Delta_T/H$ ) at the roof of the building, where H is the total height of the multistory building. This dimensionless ratio shows the effect of the earthquake records on the roof drift of the RC building frames in relation to its total height. Table 3 show the percentage of target drift ratios for the multistory RC building frames. The results include the modal drift ratios for the first three modes of vibration. The total target drift ratio of the RC frame is determined by combining the modal drift ratios using the standard SRSS rule, and listed in the tables in the last column under SRSS heading. It is noticed that the effect of higher modes of vibration on the target drift ratios is not very significant for. This is expected as the studied RC building frames are regular type.

For each target drift value, the corresponding value of the base shear at the foundation level is determined by the MPA method. The results are expressed as the base shear ratio ( $V_{bT}/W$ ), which is a dimensionless value. The base shear values for the different RC buildings are illustrated in table 4 using the four studied earthquakes. The base shear is not influenced by the higher modes of vibration as the results indicate.

### 5.1.2 Floor displacement profiles

The lateral displacements at each floor level are determined at the target drift of each modal lateral load pattern. Each floor displacement is divided by the total height of the multistory building to be expressed using a dimensionless value. Figs.12 and 13 show the floor displacement profiles determined using the lateral load pattern for each of the first three modes of vibration. For some cases, it is noticed that the final profile of the floor displacements almost coincides with the modal profile based on the first mode.

**Table 3:** Percentage of target drift ( $\Delta_T/H$ ) by MPA due to the four studied earthquakes

(a) ALTADENA earthquake.

RC Building Frame	Mode 1	Mode 2	Mode 3	SRSS
6-story, 3-bay	0.7342	0.0240	0.0044	0.7350
12-story, 3-bay	0.3054	0.0193	0.0071	0.3061

(b) CORRALIT earthquake.

RC Building Frame	Mode 1	Mode 2	Mode 3	SRSS
6-story, 3-bay	1.0688	0.0700	0.0066	1.0711
12-story, 3-bay	0.7346	0.0992	0.0165	0.7414

(c) POMONA earthquake.

RC Building Frame	Mode 1	Mode 2	Mode 3	SRSS
6-story, 3-bay	0.1643	0.0575	0.0115	0.1744
12-story, 3-bay	0.1550	0.0163	0.0121	0.1563

(d) LACC-NOR earthquake.

RC Building Frame	Mode 1	Mode 2	Mode 3	SRSS
6-story, 3-bay	0.5338	0.0369	0.0076	0.5350
12-story, 3-bay	0.2790	0.0283	0.0117	0.2806

**Table 4:** Target base-shear ratio ( $V_{bT}/W$ ) by MPA due to the four studied earthquakes

(a) ALTADENA earthquake.

RC Building Frame	Mode 1	Mode 2	Mode 3	SRSS
6-story, 3-bay	0.1708	0.0268	0.0049	0.1720
12-story, 3-bay	0.1510	0.0130	0.0047	0.1520

(b) CORRALIT earthquake.

RC Building Frame	Mode 1	Mode 2	Mode 3	SRSS
6-story, 3-bay	0.2161	0.0681	0.0073	0.22
12-story, 3-bay	0.2095	0.1051	0.0175	0.2350

(c) POMONA earthquake.

RC Building Frame	Mode 1	Mode 2	Mode 3	SRSS
6-story, 3-bay	0.1159	0.0606	0.0128	0.13
12-story, 3-bay	0.1084	0.0111	0.0082	0.1093

(d) LACC-NOR earthquake.

RC Building Frame	Mode 1	Mode 2	Mode 3	SRSS
6-story, 3-bay	0.1352	0.0411	0.0084	0.14
12-story, 3-bay	0.1130	0.0192	0.0079	0.1149

### 5.1.3 Inter-story Seismic Drifts

The inter-story drift ratio (IDR) is defined as the difference between the total lateral displacements of two successive floors divided by the floor height between them, as follows:

$$IDR = \frac{\Delta_i - \Delta_{i-1}}{h_i} \quad (30)$$

Where  $\Delta_i$  and  $\Delta_{i-1}$  are the total lateral displacements of  $i$  floor and  $i-1$  floor, respectively, and  $h_i$  is the floor height. Figs. 14 and 15 show the inter-story drift ratios (IDR) for the RC building frames, considering the three modal lateral load patterns of the first three modes of vibration. The final IDR values are presented by the SRSS curves. The peak values of the IDR occur near the mid-height of the RC building frame. The results of the IDR illustrate that the higher modes of vibration have significantly lesser influence on the IDR, Table 6.

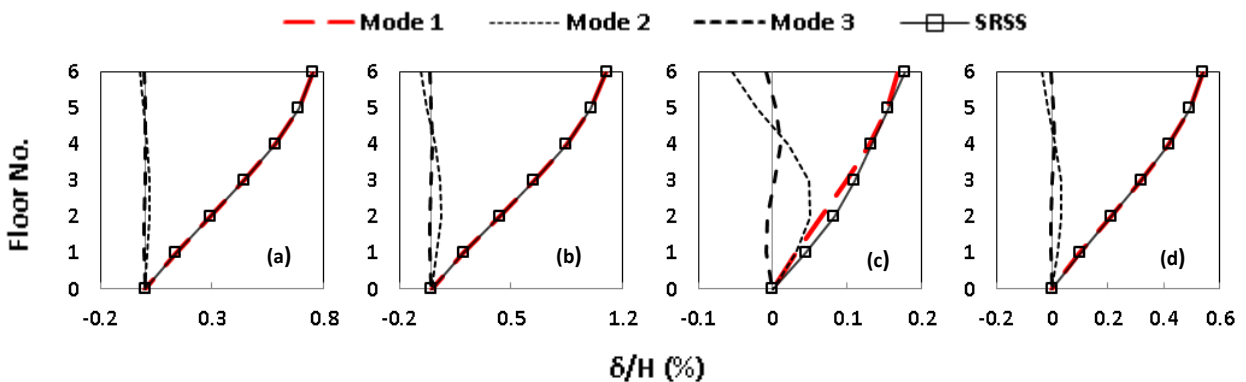


**Fig.12** Floor displacements of 6-story frame determined by (MPA) due to (a) ALTADENA, (b) CORRALIT, (c) POMONA and (d) LACC-NOR earthquakes.

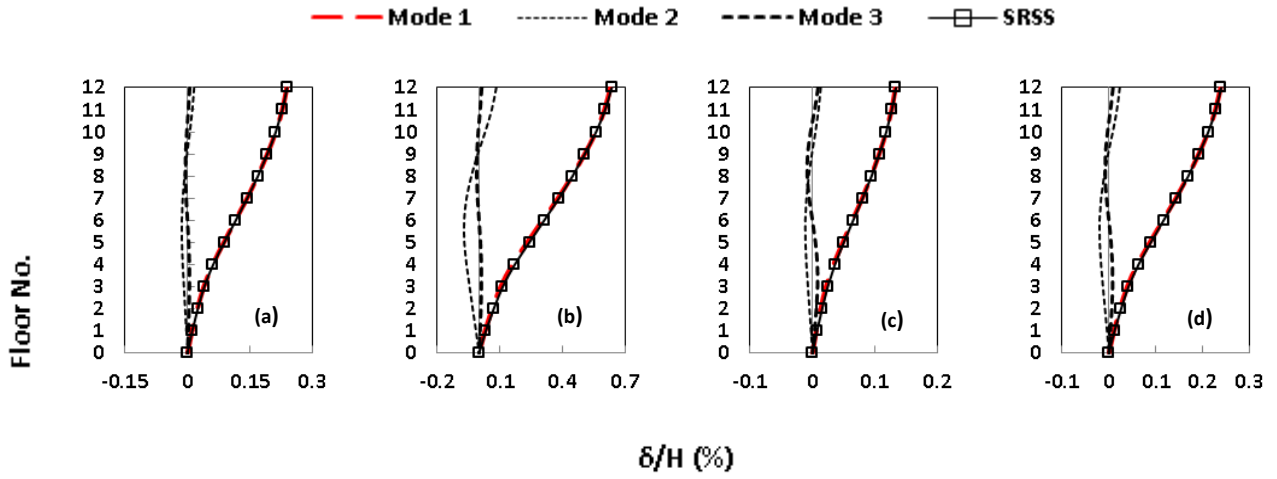


**Fig.13** Floor displacements of 12-story frame determined by (MPA) due to (a) ALTADENA, (b) CORRALIT, (c) POMONA and (d) LACC-NOR earthquakes.

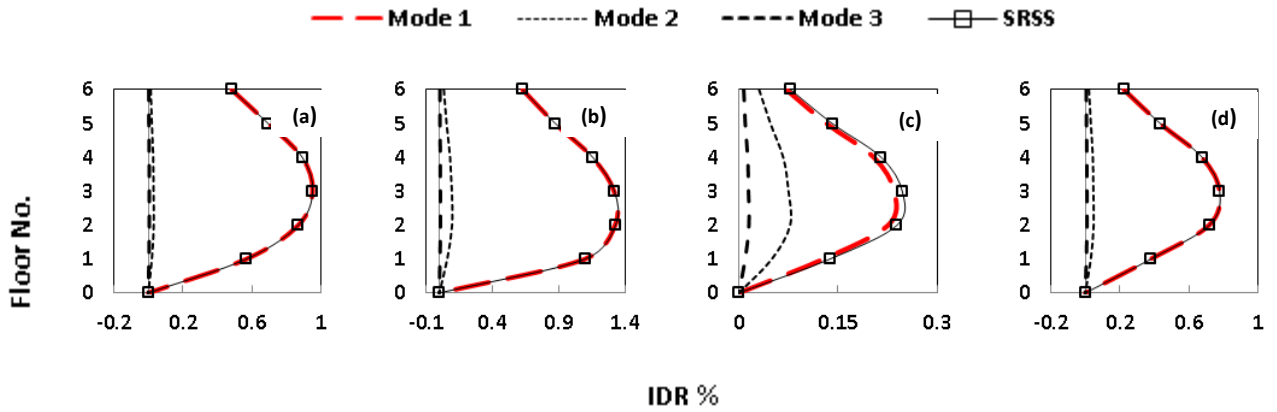


**Fig.14** (IDR) of 6-story frame determined by (MPA) due to (a) ALTADENA, (b) CORRALIT, (c) POMONA and (d) LACC-NOR earthquakes.

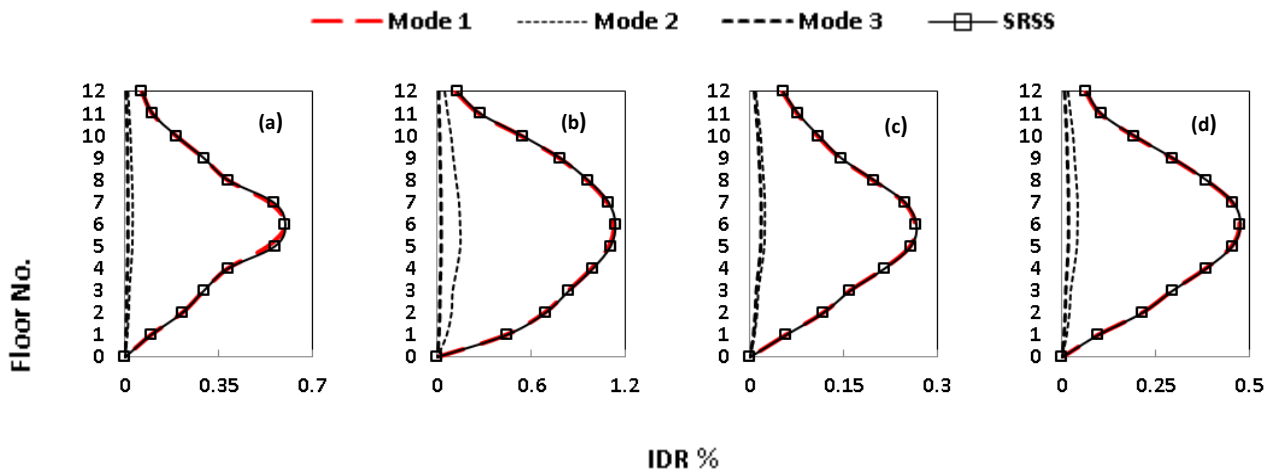


**Fig.15** (IDR) of 12-story frame determined by (MPA) due to (a) ALTADENA, (b) CORRALIT, (c) POMONA and (d) LACC-NOR earthquakes.

**Table 5:** Peak Inter-story drift ratio (IDR) by MPA due to the four studied earthquakes.

(a) ALTADENA earthquake.					(b) CORRALIT earthquake.				
RC Building Frame	Mode 1	Mode 2	Mode 3	SRSS	RC Building Frame	Mode 1	Mode 2	Mode 3	SRSS
6-story, 3-bay	0.9523	0.0316	0.0061	0.9528	6-story, 3-bay	1.3257	0.0969	0.009	1.32
12-story, 3-bay	0.6	0.0281	0.0104	0.6	12-story, 3-bay	1.1295	0.1466	0.02439	1.14

(c) POMONA earthquake.					(d) LACC-NOR earthquake.				
RC Building Frame	Mode 1	Mode 2	Mode 3	SRSS	RC Building Frame	Mode 1	Mode 2	Mode 3	SRSS
6-story, 3-bay	0.2352	0.0777	0.0154	0.2481	6-story, 3-bay	0.778	0.0483	0.0102	0.77
12-story, 3-bay	0.2652	0.0236	0.0176	0.2668	12-story, 3-bay	0.4749	0.0412	0.0170	0.47

## 5.2 Comparison between NLTH (SAP2000), NLTH (MATLAB), N2 and MPA Characteristics

In principle, the nonlinear time-history analysis (NLTH) is considered the most accurate method of analysis for estimating the seismic responses. The NLTH is performed using SAP2000 and MATLAB programs on the 6-story and 12-story building frames. All the results of the seismic responses determined by the MPA and N2 methods are compared with the corresponding results determined by the NLTH using SAP2000 and MATLAB programs. This comparison validates the accuracy of the MPA and N2 methods when applied to the RC building frames.

### 5.2.1 Target drift ratio and base shear

The target drift is the peak roof drift of the RC building frame when it is subjected to the action of the earthquake. Tables 7 show the percentage of target drift ratios ( $\Delta_T/H$ ) determined by the NLTH (SAP2000 & MATLAB), N2 and MPA methods. Also, the ratios of these values related to NLTH (SAP2000) are listed. These ratios show the accuracy of the N2 and MPA methods, where a value of 1.0 indicates that the results of these methods are identical to the NLTH (SAP2000) results, a value  $<1.0$  indicates that the results of these methods are not conservative compared to the NLTH (SAP2000) results, and a value  $>1.0$  indicates that the results of these methods are conservative.

In general, the roof drift ratios resulting from N2 and MPA methods achieve acceptable convergence for the same ratios resulting from NLTH (SAP2000 & MATLAB) analyses methods, where the differences of these ratios are ranging from 0% to 5%. The N2 method gives the most conservative results for the target drift compared to NLTH (SAP2000). However the MPA method occupies the second state. But the MPA yields un-conservative values for the target drift by about -3% in most cases. The NLTH (SAP2000) method gives the most convergent results for the target drift compared to MPA and N2. However the NLTH (MATLAB) method occupies the second state. And this returns to the similarity of the nonlinearity concepts of MPA, N2 and NLTH

(SAP2000) applications in this study. On the other hand, the degree of convergence of the all methods to determine the target drift ratios is sufficiently strong, as shown by the results from through Table 6. This accuracy is acceptable for design purposes, as that the estimated target drift is conservative. Table 7 shows the percentage of base-shear ratio ( $V_{bT}/W$ ). The results indicate that the MPA method provides values of  $V_{bT}/W$  to some extent close to those determined by using the NLTH (SAP2000) method.

**Table 6** percentage of target drift ratio ( $\Delta_T/H$ ) of the studied RC frames determined by (NLTH-SAP2000), (NLTH-MATLAB), (N2) and (MPA) due to the four studied earthquakes.

(a) ALTADENA earthquake

		NLTH (SAP2000)	NLTH (MATLAB)	MPA	N2
6-story, 3-bay	$\Delta_{max}/H$	0.74	0.7368	0.73	0.74
	Value relative to NLTH-SAP	1	0.99	0.99	1
12-story, 3-bay	$\Delta_{max}/H$	0.31	0.32	0.30	0.33
	Value relative to NLTH-SAP	1	1.03	0.97	1.07

(b) CORRALIT earthquake

		NLTH (SAP2000)	NLTH (MATLAB)	MPA	N2
6-story, 3-bay	$\Delta_{max}/H$	1.09	1.05	1.07	1.05
	Value relative to NLTH-SAP	1	0.97	0.98	0.97
12-story, 3-bay	$\Delta_{max}/H$	0.76	0.7568	0.74	0.77
	Value relative to NLTH-SAP	1	0.99	0.97	1.01

(c) POMONA earthquake

		NLTH (SAP2000)	NLTH (MATLAB)	MPA	N2
6-story, 3-bay	$\Delta_{max}/H$	0.1789	0.18	0.17	0.189
	Value relative to NLTH-SAP	1	1.02	0.97	1.05
12-story, 3-bay	$\Delta_{max}/H$	0.1630	0.1676	0.16	0.167
	Value relative to NLTH-SAP	1	1.02	0.96	1.02

(d) LACC-NOR earthquake

		NLTH (SAP2000)	NLTH (MATLAB)	MPA	N2
6-story, 3-bay	$\Delta_{max}/H$	0.539	0.57	0.535	0.536
	Value relative to NLTH-SAP	1	1.05	0.99	1.05
12-story, 3-bay	$\Delta_{max}/H$	0.27	0.29	0.28	0.27
	Value relative to NLTH-SAP	1	1.07	1.03	1

**Table 7:** Target base-shear ratio ( $V_{bT}/W$ ) of the studied RC frames determined by (NLTH-SAP2000), (NLTH-MATLAB) and (MPA) due to the four studied earthquakes.

(a) ALTADENA earthquake

		NLTH (SAP2000)	NLTH (MATLAB)	MPA	N2
6-story, 3-bay	$V_{bT}/W$	0.1721	0.16	0.172	0.171
	Value relative to NLTH-SAP	1	0.93	1	0.99
12-story, 3-bay	$V_{bT}/W$	0.16	0.15	0.152	0.151
	Value relative to NLTH-SAP	1	0.95	0.95	0.94

(b) CORRALIT earthquake

		NLTH (SAP2000)	NLTH (MATLAB)	MPA	N2
6-story, 3-bay	$V_{bT}/W$	0.2062	0.22	0.22	0.216
	Value relative to NLTH-SAP	1	1.06	1.06	1.04
12-story, 3-bay	$V_{bT}/W$	0.24	0.24	0.235	0.22
	Value relative to NLTH-SAP	1	1	0.98	0.92

(c) POMONA earthquake

		NLTH (SAP2000)	NLTH (MATLAB)	MPA	N2
6- story, 3-bay	$V_{bT}/W$	0.13	0.127	0.13	0.12
	Value relative to NLTH-SAP	1	0.98	1	0.94
12- story, 3-bay	$V_{bT}/W$	0.11	0.1	0.109	0.108
	Value relative to NLTH-SAP	1	0.91	0.99	0.98

(d) LACC-NOR earthquake

		NLTH (SAP2000)	NLTH (MATLAB)	MPA	N2
6- story, 3-bay	$V_{bT}/W$	0.1448	0.13	0.142	0.135
	Value relative to NLTH-SAP	1	0.93	0.98	0.93
12- story, 3-bay	$V_{bT}/W$	0.11	0.1	0.114	0.113
	Value relative to NLTH-SAP	1	0.91	1.04	1.02

### 5.2.2 Floor displacements

Figs 16 and 17 show the results of floor lateral displacements. The floor lateral displacements determined by N2 are the closest for those determined by the NLTH-SAP2000 as it is clearly appeared in the figures. According to that the first mode shape of the studied building frames is the most effective mode for the values of the floor lateral displacements as was clear from the MPA results, so the floor lateral displacements determined by NLTH-SAP2000 are between those determined by the N2 and the MPA, Where the N2 method mainly depends on the first mode shape. However the floor lateral displacements determined by NLTH-MATLAB are the closest for those determined by the NLTH-SAP2000, as it is clearly appeared in the diagrams.

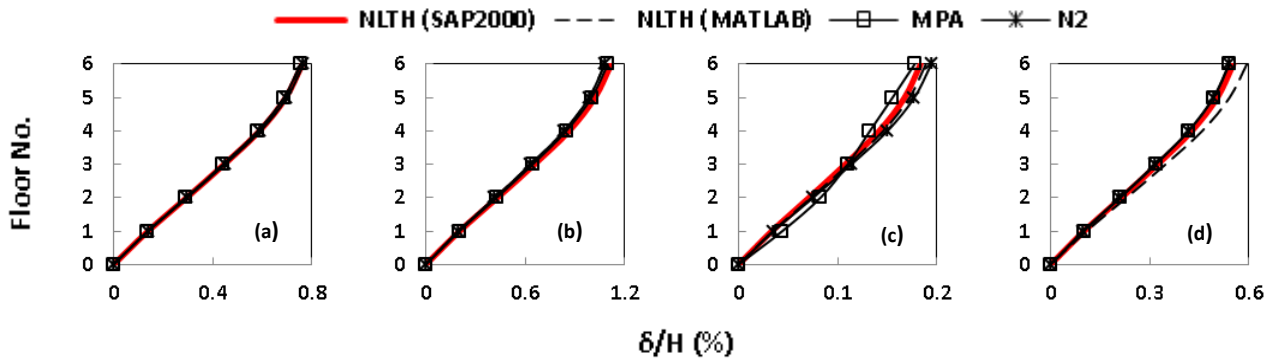


Fig.16: Floor disp. of 6-story frame due to (a) ALTADENA, (b) CORRALIT, (c) POMONA and (d) LACC-NOR earthquakes.

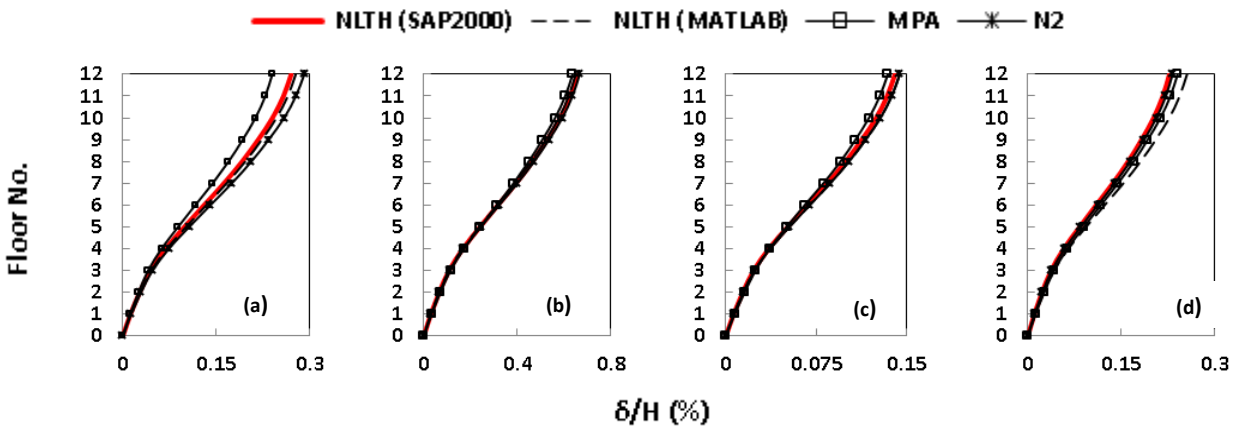


Fig.17 Floor disp. of 12-story frame due to (a) ALTADENA, (b) CORRALIT, (c) POMONA and (d) LACC-NOR earthquakes.

### 5.2.3 Comparisons of inter-story seismic drifts

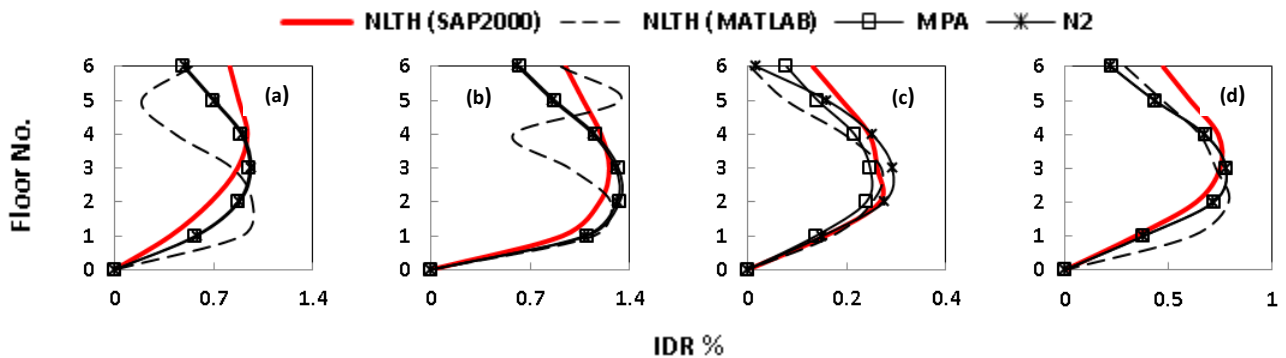
Figs.18 and 19 show the inter-story drift ratios (IDR) along the height of the RC building frames. The N2 and MPA methods have clearly convergent results for the IDR, but at the same time the IDR results of the both methods are not sufficiently convergent relative to the NLTH-SAP2000 informed that the NLTH-SAP2000 is the most accurate method. The N2 method can be applied for estimating the inter-story drifts of the multistory RC building frames because it gives results that are, in general, higher than those of the NLTH and are also conservative for design purposes. Table 8 show the peak inter-story drift ratios (IDR). For the inter-story drift ratios (IDR) determined by the NLTH-Matlab and NLTH-Sap2000 methods, clearly appear lack in the convergence between them due to the difference in the used concept of each program.

**Table 8** Peak Inter-story drift ratio (IDR) of the studied RC frames determined by (NLTH-SAP2000), (NLTH-MATLAB), (MPA) and N2 due to the four studied earthquakes.

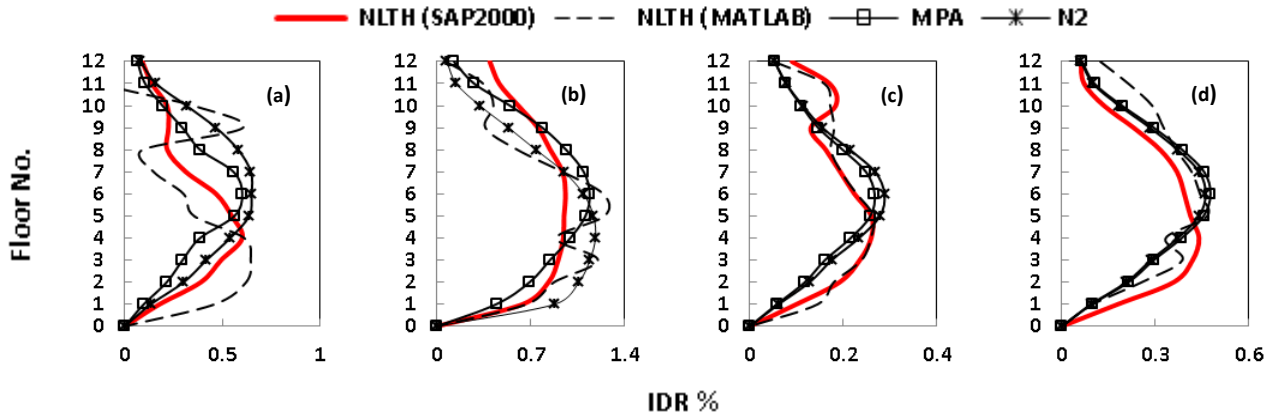
		(a) ALTADENA earthquake				(b) CORRALIT earthquake			
		NLTH (SAP2000)	NLTH (MATLAB)	MPA	N2	NLTH (SAP2000)	NLTH (MATLAB)	MPA	N2
6-story, 3-bay	IDR	0.94	0.97	0.952	0.96	1.26	1.26	1.32	1.30
	Value relative to NLTH-SAP	1	1.03	1.01	1.02	1	1	1.05	1.04
12-story, 3-bay	IDR	0.6	0.64	0.6	0.64	1.2	1.25	1.13	1.18
	Value relative to NLTH-SAP	1	1.07	1	1.08	1	1.04	0.95	0.99

		(c) POMONA earthquake				(d) LACC-NOR earthquake			
		NLTH (SAP2000)	NLTH (MATLAB)	MPA	N2	NLTH (SAP2000)	NLTH (MATLAB)	MPA	N2
6-story, 3-bay	IDR	0.267	0.27	0.25	0.29	0.75	0.79	0.77	0.77
	Value relative to NLTH-SAP	1	1.01	0.94	1.08	1	1.05	1.03	1.03
12-story, 3-bay	IDR	0.26	0.265	0.266	0.28	0.44	0.46	0.476	0.46
	Value relative to NLTH-SAP	1	1.01	1.02	1.07	1	1.06	1.08	1.04



**Fig.18** IDR of 6-story frame due to (a) ALTADENA, (b) CORRALIT, (c) POMONA and (d) LACC-NOR earthquakes.



**Fig.19** IDR of 6-story frame due to (a) ALTADENA, (b) CORRALIT, (c) POMONA and (d) LACC-NOR earthquakes.

### 5.2.3 Comparison of plastic hinge distributions

The plastic hinge distribution of the RC building frames can be viewed as a good indication of the amount of damage that is expected to occur in case of the applied seismic action. Figs. 20 and 21 show the diagrams of the plastic hinges distributions in both the studied RC building frames resulting from, the NLTH (Sap2000) procedure and the inelastic pushover analysis through the N2 procedure. The results in these figures for the studied building show that:

- 1- For almost cases, damage level determined by NLTH (Sap2000) procedure is approximated to that damage level resulting from the pushover analysis.
- 2- The results of damage level are expected for every studied earthquake ground acceleration records due to different intensity levels for these selected earthquakes and their frequency contents relative to the dynamic characteristic of the building.

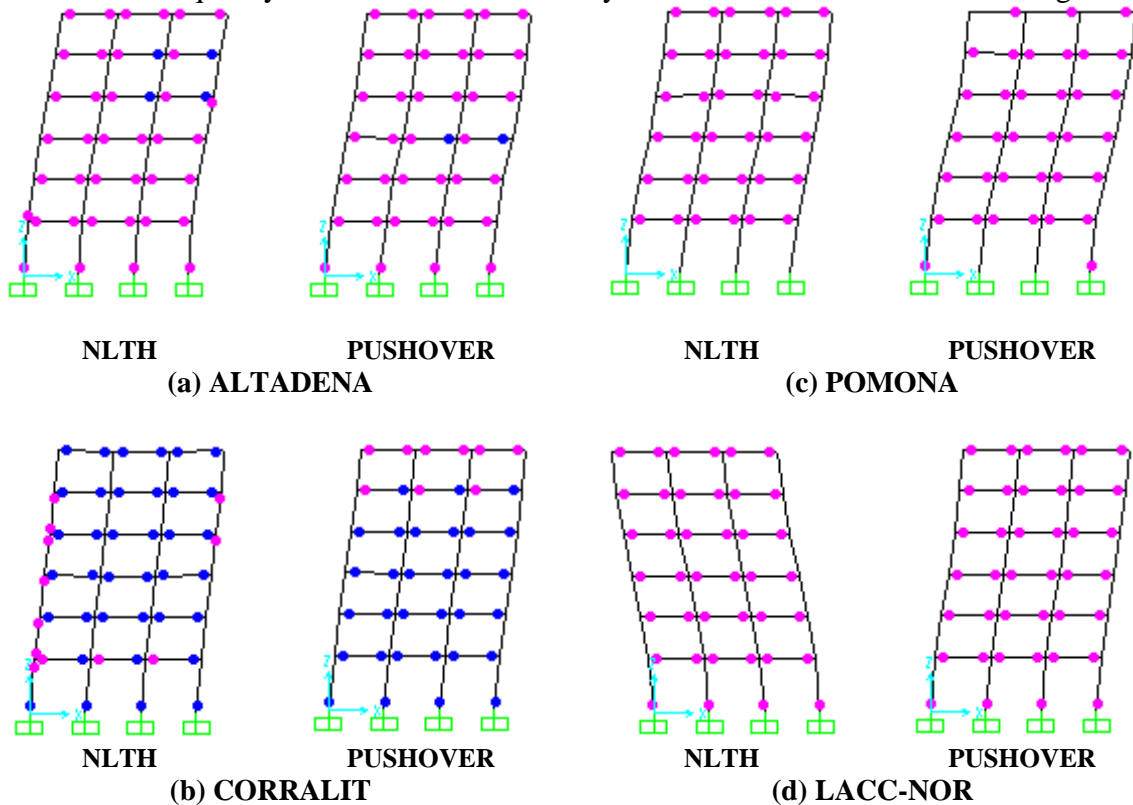


**Fig. 20:** Plastic hinges distributions due to (a) ALTADENA, (b) CORRALIT, (c) POMONA and (d) LACC-NOR earthquakes and N2 method. (6-story)

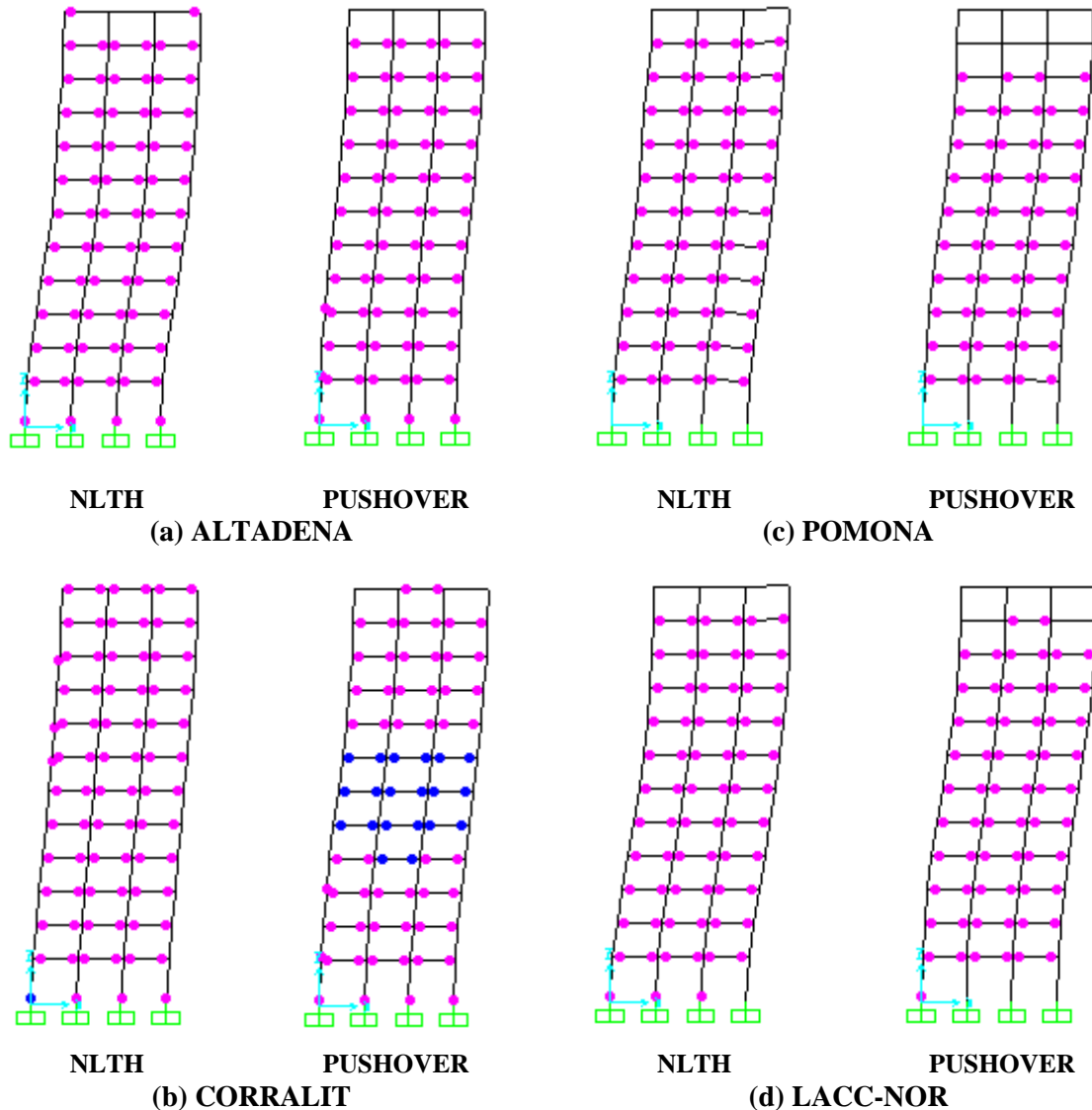


**Fig. 21:** Plastic hinges distributions due to (a) ALTADENA, (b) CORRALIT, (c) POMONA and (d) LACC-NOR earthquakes and N2 method. (12-story)

### 5.3 The Effect of Lateral Load Patterns on the N2 Method Results

#### 5.3.1 Evaluation of the Global Behavior of the Models

As mentioned before, five lateral load patterns are utilized in the nonlinear static pushover analyses through the N2 method. Table 9 shows the percentage of target drift ratios ( $\Delta_T/H$ ). The ratios between the results of the five lateral load patterns and the NLTH-SAP2000 are listed. These ratios show the accuracy of the N2 method using various lateral load patterns.

Table 10 shows the percentage of base-shear ratio ( $V_{bT}/W$ ). It is observed that the L.L.P5 is the most lateral load pattern type achieves the lowest base shear and roof displacement values in the two cases of the two studied RC frames. This is certainly as a result of that the L.L.P5 has some negative values of the lateral loads beside the positive values, while the all rest studied lateral load patterns types has only positive values of the lateral loads. In general, it is clearly observed that the lateral load patterns types which depend on the mode shape values give closer values to that of the NLTH. While,

the proposed lateral load patterns types achieve somewhat unclosed values compared to that of the NLTH in many times. Where, these both proposed types' functions depend only on the height (H) of the studied frame.

### 5.3.2 Story Displacements

In Figs 22 and 23, the story displacement diagrams obtained for the two RC building frames; are given for the five lateral load pattern cases through the N2 method, compared with the nonlinear time history analyses results. It is observed from the analyses results that the story displacements obtained from the pushover and nonlinear time history analyses are generally close to each other for the lateral load patterns types which depend on the mode shape values cases. As a special behavior, elastic first mode lateral load pattern (i.e. L.L.P3) curves are quite similar to the nonlinear time history curve in the 6-story and the 12-story cases. While, the story displacements obtained by the code lateral load pattern and the uniform lateral load pattern (i.e. L.L.P1 and L.L.P2) are generally observed to be strongly convergent. But, the proposed lateral load patterns types which their functions depend only on the height (H) of the studied frame achieve somewhat far story displacements compared to that of the NLTH in many times.

**Table 9:** Percentage of target drift ( $\Delta_T/H$ ) by N2 due to the four studied earthquakes.

		(a) ALTADENA earthquake						(b) CORRALIT earthquake						
		NLTH	L.L.P 1	L.L.P 2	L.L.P 3	L.L.P 4	L.L.P 5	NLTH	L.L.P 1	L.L.P 2	L.L.P 3	L.L.P 4	L.L.P 5	
6-story	$\Delta_{max}/H$	0.742	0.721	0.721	0.747	0.687	0.789	$\Delta_{max}/H$	1.090	1.045	1.045	1.052	0.973	1.157
	Value relative to NLTH	1	0.97	0.97	1.007	0.93	1.06	Value relative to NLTH	1	0.96	0.96	0.97	0.9	1.06
12-story	$\Delta_{max}/H$	0.314	0.297	0.297	0.338	0.310	0.378	$\Delta_{max}/H$	0.764	0.739	0.739	0.776	0.709	0.783
	Value relative to NLTH	1	0.95	0.95	1.07	0.99	1.20	Value relative to NLTH	1	0.97	0.97	1.01	0.93	1.02

		(c) POMONA earthquake						(d) LACC-NOR earthquake						
		NLTH	L.L.P 1	L.L.P 2	L.L.P 3	L.L.P 4	L.L.P 5	NLTH	L.L.P 1	L.L.P 2	L.L.P 3	L.L.P 4	L.L.P 5	
6-story	$\Delta_{max}/H$	0.178	0.190	0.190	0.189	0.175	0.210	$\Delta_{max}/H$	0.538	0.521	0.521	0.535	0.447	0.593
	Value relative to NLTH	1	1.06	1.06	1.05	0.98	1.17	Value relative to NLTH	1	0.97	0.97	0.994	0.83	1.1
12-story	$\Delta_{max}/H$	0.163	0.164	0.164	0.167	0.154	0.189	$\Delta_{max}/H$	0.270	0.259	0.259	0.272	0.230	0.297
	Value relative to NLTH	1	1.009	1.009	1.02	0.95	1.16	Value relative to NLTH	1	0.96	0.96	1.008	0.86	1.1

**Table 10:** Target base-shear ratio ( $V_{bT}/W$ ) by N2 due to the four studied earthquakes.

		(a) ALTADENA earthquake						(b) CORRALIT earthquake						
		NLTH	L.L.P 1	L.L.P 2	L.L.P 3	L.L.P 4	L.L.P 5	NLTH	L.L.P 1	L.L.P 2	L.L.P 3	L.L.P 4	L.L.P 5	
6-story	$V_{bT}/W$	0.172	0.170	0.170	0.171	0.171	0.170	$V_{bT}/W$	0.206	0.215	0.215	0.216	0.215	0.216
	Value relative to NLTH	1	0.992	0.992	0.993	0.993	0.991	Value relative to NLTH	1	1.04	1.04	1.04	1.04	1.05
12-story	$V_{bT}/W$	0.160	0.149	0.149	0.151	0.150	0.156	$V_{bT}/W$	0.240	0.216	0.216	0.220	0.214	0.229

	Value relative to NLTH	1	0.94	0.94	0.95	0.94	0.98
--	------------------------	---	------	------	------	------	------

	Value relative to NLTH	1	0.91	0.91	0.92	0.9	0.96
--	------------------------	---	------	------	------	-----	------

(c) POMONA earthquake

		NLTH	L.L.P 1	L.L.P 2	L.L.P 3	L.L.P 4	L.L.P 5
6-story	$V_{bT}/W$	0.130	0.119	0.119	0.122	0.116	0.124
	Value relative to NLTH	1	0.92	0.92	0.95	0.9	0.96
12-story	$V_{bT}/W$	0.110	0.106	0.106	0.108	0.103	0.112
	Value relative to NLTH	1	0.97	0.97	0.99	0.94	1.01

(d) LACC-NOR earthquake

		NLTH	L.L.P 1	L.L.P 2	L.L.P 3	L.L.P 4	L.L.P 5
6-story	$V_{bT}/W$	0.144	0.134	0.134	0.135	0.127	0.141
	Value relative to NLTH	1	0.93	0.93	0.94	0.9	0.98
12-story	$V_{bT}/W$	0.110	0.110	0.110	0.113	0.109	0.113
	Value relative to NLTH	1	1.003	1.003	1.02	1	1.03

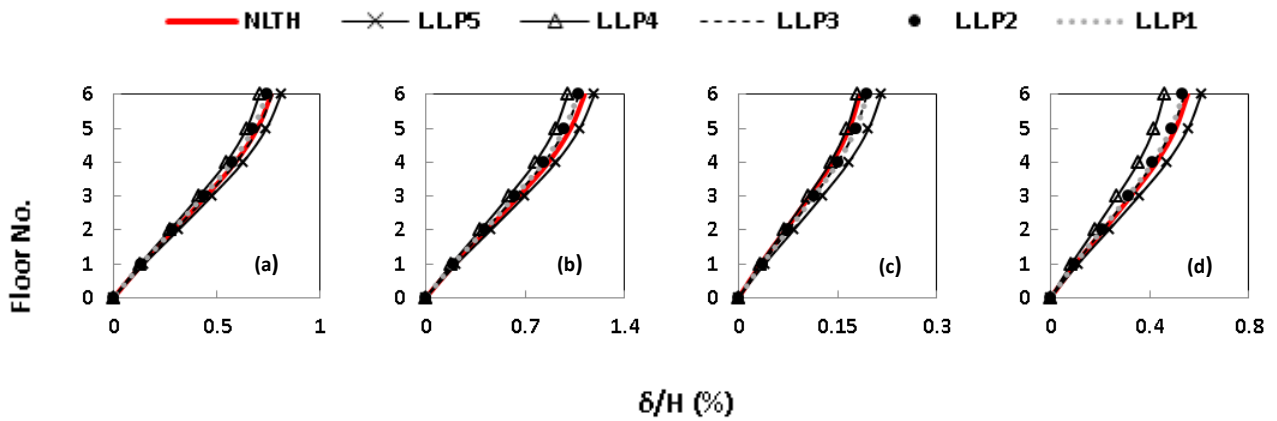


Fig.22 (Floor Disp.) of 6-story frame determined by (N2) due to (a) ALTADENA, (b) CORRALIT, (c) POMONA and (d) LACC-NOR earthquakes.

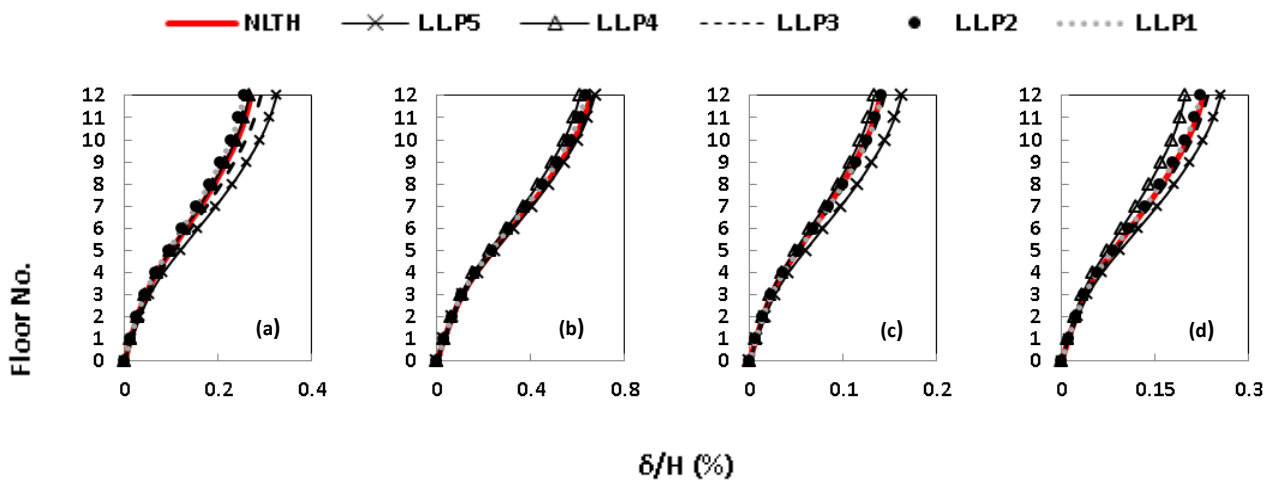


Fig.23 (Floor Disp.) of 12-story frame determined by (N2) due to (a) ALTADENA, (b) CORRALIT, (c) POMONA and (d) LACC-NOR earthquakes.

### 5.3.3 Inter-Story Drift Ratios

As an illustration, the inter-story drift ratio profiles of the 6-story and the 12-story RC building frame are given in Figs. 24 and 25, respectively. However, Table 11 shows the

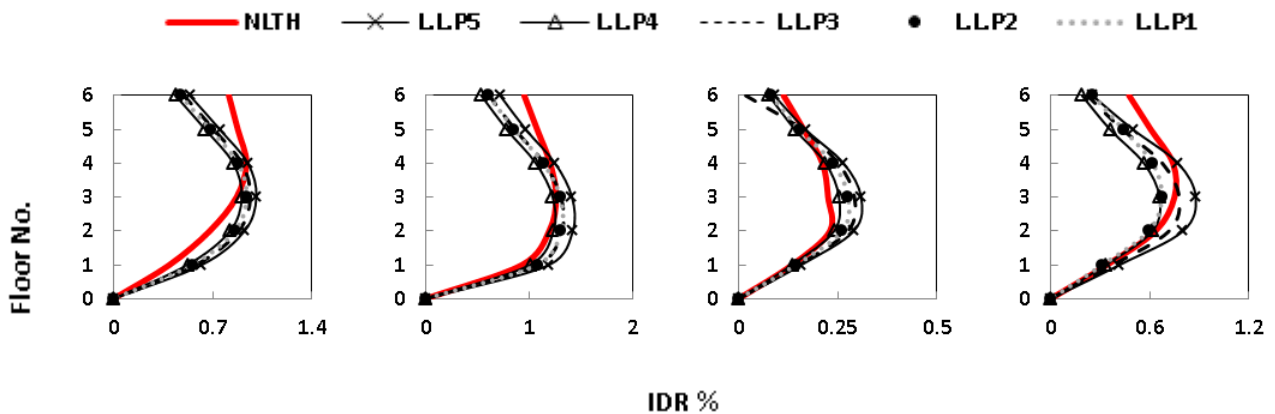
peak inter-story drift ratios. The first mode lateral load pattern predicts the inter-story drift ratios closer to those obtained by the nonlinear time history analyses. In general, all studied lateral load pattern types predict the inter-story drift ratios closer to those obtained by the nonlinear time history analyses in the case of the stories under the mid-height of the studied buildings. This is expected as the studied buildings are regular buildings.

**Table 11:** Peak Inter-story drift ratio (IDR) by N2 due to the four studied earthquakes.

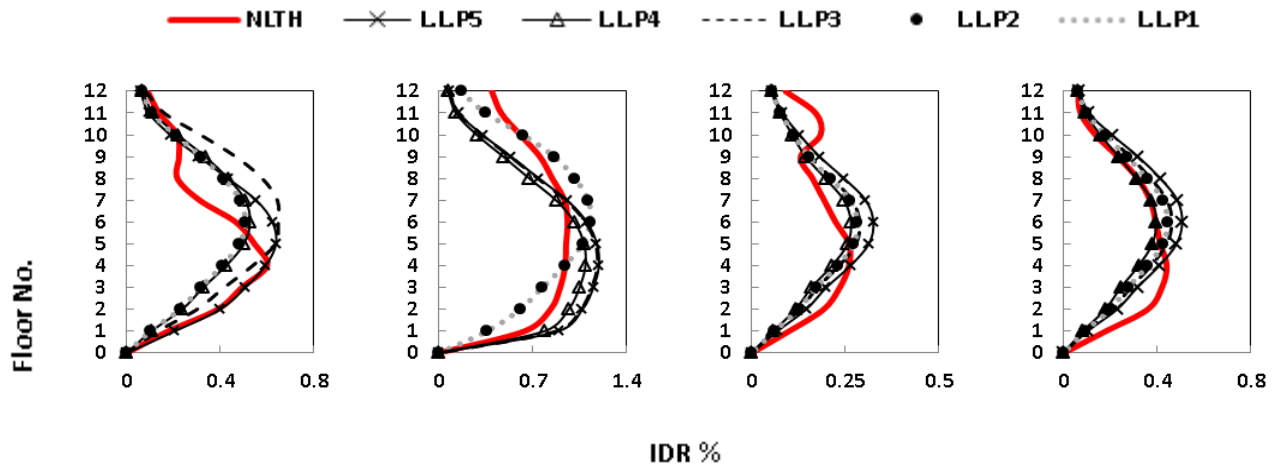
		(a) ALTADENA earthquake						(b) CORRALIT earthquake					
		NLTH	L.L.P 1	L.L.P 2	L.L.P 3	L.L.P 4	L.L.P 5	NLTH	L.L.P 1	L.L.P 2	L.L.P 3	L.L.P 4	L.L.P 5
6-story	IDR	0.937	0.939	0.939	0.965	0.905	1.008	1.256	1.302	1.302	1.309	1.230	1.415
	Value relative to NLTH	1	1.002	1.002	1.02	0.97	1.07	1	1.03	1.03	1.04	0.98	1.12
12-story	IDR	0.600	0.485	0.485	0.648	0.527	0.637	1.200	1.127	1.127	1.182	1.092	1.192
	Value relative to NLTH	1	0.81	0.81	1.080	0.9	1.06	1	0.97	0.97	0.99	0.91	0.994

		(c) POMONA earthquake						(d) LACC-NOR earthquake					
		NLTH	L.L.P 1	L.L.P 2	L.L.P 3	L.L.P 4	L.L.P 5	NLTH	L.L.P 1	L.L.P 2	L.L.P 3	L.L.P 4	L.L.P 5
6-story	IDR	0.267	0.276	0.276	0.290	0.253	0.309	0.750	0.672	0.672	0.778	0.659	0.878
	Value relative to NLTH	1	1.03	1.03	1.08	0.96	1.15	1	0.9	0.9	1.03	0.9	1.17
12-story	IDR	0.260	0.282	0.282	0.280	0.264	0.324	0.440	0.443	0.44	0.461	0.394	0.506
	Value relative to NLTH	1	1.08	1.08	1.07	1.01	1.20	1	1.007	1.007	1.04	0.9	1.15



**Fig.24:** (IDR) of 6-story frame determined by (N2) due to (a) ALTADENA, (b) CORRALIT, (c) POMONA and (d) LACC-NOR earthquakes.



**Fig. 25:** (IDR) of 12-story frame determined by (N2) due to (a) ALTADENA, (b) CORRALIT, (c) POMONA and (d) LACC-NOR earthquakes.

## 6. CONCLUSIONS

The results of the present investigation support the following conclusions:

- 1- Comparing the results obtained by using MPA procedure with the same results of the nonlinear time-history analysis (NLTH) indicated that MPA method has reliable efficiency and acceptable accuracy in estimating floor displacements, story drifts, plastic hinge rotations and plastic hinge locations.
- 2- The use of the pushover analysis methods (MPA and N2) with invariant lateral force distribution as an alternative method for the NLTH, overcomes the complications appear in necessary providing the actual ground acceleration values of an intended site for representing the required seismic force in the analysis by using the NLTH method.
- 3- The utilizing of MATLAB in programming the nonlinear time-history analysis procedure achieves acceptable accuracy and efficiency.
- 4- The use of the lateral load pattern with the first mode shape of the studied buildings has the most effect on the MPA results, compared to the other lateral load patters with the second or the third mode shapes of the same building. This is expected as the studied buildings are regular buildings.
- 5- The damage level determined by pushover analysis of the N2 method is approximated to that damage level resulting from the NLTH (Sap2000) procedure. The results of damage level are expected for each studied case due to different intensity level for the selected earthquake ground acceleration records and their frequency contents relative to the dynamic characteristic of the building.
- 6- The shape choice of the applied lateral load pattern affects the efficiency of the N2 method. Through this study, it is proved that the lateral load patterns types which depend on the mode shape values give closer values to that of the NLTH.

## 7. REFERENCES

- Abbasnia, R., Davoudi, A.T. and Maddah, M.M. (2013). "An adaptive pushover procedure based on effective modal mass combination rule", *Engineering Structures* 52, 654-666.
- Abd-El-Wahab, M.M., (2008) "Determination of Inelastic Seismic Responses for Mid-Rise RC Buildings by Modal Pushover Analysis", M.Sc. Thesis, Civil Engineering Department, Faculty of Engineering, Cairo University, Egypt.

- Altuntop, M.N., (2007) "Analysis of Building Structures with Soft Stories", M.Sc. Thesis, Civil Engineering Department, Faculty of Engineering, Atilim University, Turkey.
- Amini, M.A. and Poursha, M. (2016) "A non-adaptive displacement-based pushover procedure for the nonlinear static analysis of tall building frames", *Engineering Structures*, 126, 586-597.
- ATC 40, (1996) "Seismic Evaluation and Retrofit of Concrete Buildings", Applied Technology Council, Volume 1-2, California.
- Beheshti-Aval, S.B. and Keshani, S. (2014) "A Phenomenological study on inelastic torsion caused by nonlinear behavior changes during earthquake excitations", *Civil Engineering Infrastructures Journal*, 47(2), 273-290.
- Camara, A. and Astiz, M. (2012) "Pushover analysis for the seismic response prediction of cable-stayed bridges under multi-directional excitation", *Engineering Structures*, 41, 444-455.
- Chopra A. K. and Goel R. K., A modal pushover analysis procedure to estimate seismic demands for buildings: Summary and Evaluation, Fifth National Conference on Earthquake Engineering, 26-30 May 2003, Istanbul, Turkey.
- Eberhard M.O. and Sözen M.A., (1993) "Behavior-Based Method to Determine Design Shear in Earthquake Resistant Walls", *Journal of the Structural Division, American Society of Civil Engineers*, New York, Vol.119, No.2, (619-640),.
- ECP-201, (2012) Egyptian Code for Calculating Loads and Forces in Structural Work and Masonry, National Research Center for Housing and Building, Giza, Egypt.
- ECP-203, (2007) Egyptian Code for Design and Construction of Reinforced Concrete Structures, National Research Center for Housing and Building, Giza, Egypt.
- EN 1998-1 (2004) Eurocode 8, Design provisions for earthquake resistance of structures, Part 1: General rules, seismic actions and rules for buildings, European Committee for Standardization, Brussels.
- Fajfar, P. (2000) "A nonlinear analysis method for performance based seismic design," *Earthquake Spectra* 16[3], 573-592.
- Fajfar, P. and Fischinger M., (1987) "Nonlinear Seismic Analysis of R/C Buildings: Implications of a Case Study", *European Earthquake Engineering*, Vol.1, (31-43),
- FEMA 356 (2000) Pre-standard and Commentary for the Rehabilitation of Buildings.
- FEMA-273 (1997) NEHRP Guidelines for the Seismic Rehabilitation of Buildings,
- FEMA 440 (2005) Improvement of nonlinear static seismic analysis procedures, Prepared for: Department of Homeland Security Federal Emergency Management Agency, Washington, D.C.
- Freeman S.A., Mahaney J.A., Paret T.F. and Kehoe B.E., (1993) "The Capacity Spectrum Method for Evaluating Structural Response During the Loma Prieta

- Earthquake”, National Earthquake Conference, Central U.S. Earthquake Consortium, Tennessee, 501-510.
- Giorgi, P. and Scotta, R. (2013) "Validation and improvement of N1 method for pushover analysis", *Soil Dynamics and Earthquake Engineering*, 55, 140-147.
- Jiang, Y., Li, G. and Yang, D. (2010) "A modified approach of energy balance concept based multimode pushover analysis to estimate seismic demands for buildings", *Engineering Structures*, 32(5), 1272-1283.
- Khoshnoudian, F. and Kashani, M.M.B. (2012). "Assessment of modified consecutive modal pushover analysis for estimating the seismic demands of tall buildings with dual system considering steel concentrically braced frames”, *Journal of Constructional Steel Research*, 72, 155-167.
- Kunnath, S. K. and Kalkan, E. (2004) "Evaluation of seismic deformation demands using nonlinear procedures in multistory steel and concrete moment frames", *ISET Journal of Earthquake Technology*, 41(1), 159-181.
- Malekzadeh, H. (2013) "Response modification factor of coupled steel shear walls", *Civil Engineering Infrastructures Journal*, 46(1), 15-26.
- Manoukas, G., Athanatopoulou, A. and Avramidis, I. (2012) "Multimode pushover analysis for asymmetric buildings under biaxial seismic excitation based on a new concept of the equivalent single degree of freedom system", *Soil Dynamics and Earthquake Engineering*, 38, 88-96.
- Mario Paz, William Leigh, (2003) “Structural Dynamics - Theory and computation”, Fifth Edition, September, United States of America.
- Mazza, F. (2014) "Modelling and nonlinear static analysis of reinforced concrete framed buildings irregular in plan", *Engineering Structures*, 80, 98-108.
- Moghaddam A.S., (2002) “A Pushover Procedure for Tall Buildings”, 12th European Conference on Earthquake Engineering.
- Mwafy A.M. and Elnashai A.S., (2001) “Static Pushover versus Dynamic Analysis of R/C Buildings”, *Engineering Structures*, Vol. 23, 407-424.
- Nguyen, A.H., Chintanapakdee, C. and Hayashikawa, T. (2010) "Assessment of current nonlinear static procedures for seismic evaluation of BRBF buildings", *Journal of Constructional Steel Research*, 66(8), 1118-1127.
- Panyakapo, P. (2014) "Cyclic pushover analysis procedure to estimate seismic demands for buildings", *Engineering Structures*, 66, 10-23.
- Poursha, M., Khoshnoudian, F. and Moghadam, A. (2014) "The extended consecutive modal pushover procedure for estimating the seismic demands of two-way unsymmetrical-plan tall buildings under influence of two horizontal components of ground motions", *Soil Dynamics and Earthquake Engineering*, 63, 162-173.
- Shakeri, K., Tarbali, K. and Mohebbi, M. (2012) "An adaptive modal pushover procedure for asymmetric-plan buildings", *Engineering Structures*, 36, 160-172.